

1 **5-Deoxyadenosine Salvage by Promiscuous Enzyme Activity**
2 **leads to Bioactive Deoxy-Sugar Synthesis in**
3 ***Synechococcus elongatus***

4
5 **Running title: Unusual 5-deoxyadenosine salvage in *S. elongatus***

6
7 Johanna Rapp^a, Pascal Rath^b, Joachim Kilian^c, Klaus Brilisauer^a, Stephanie Grond^b, Karl
8 Forchhammer^{a#}

9 ^aInterfaculty Institute of Microbiology and Infection Medicine, Microbiology/Organismic Interactions, Eberhard
10 Karls Universität Tübingen, Auf der Morgenstelle 28, 72076 Tübingen, Germany.

11 ^bInstitute of Organic Chemistry, Eberhard Karls Universität Tübingen, Auf der Morgenstelle 18, 72076 Tübingen,
12 Germany.

13 ^cCenter for Plant Molecular Biology, Eberhard Karls Universität Tübingen, Auf der Morgenstelle 32, 72076
14 Tübingen, Germany.

15
16 #corresponding author (karl.forchhammer@uni-tuebingen.de, Tel.: +49 (7071) 29- 72096)

17
18 **Abbreviations:** SAM: S-Adenosylmethionine; MTA: Methylthioadenosine; 5dAdo:
19 5-Deoxyadenosine; MSP: Methionine salvage pathway; 5dR: 5-Deoxyribose; 7dSh:
20 7-Deoxysedoheptulose; 5dR-1P: 5-Deoxyribose 1-phosphate; 5dRu-1P: 5-Deoxyribulose
21 1-phosphate; MTRI: Methylthioribose 1-phosphate isomerase; MTR: Methylthioribose

22
23 **Keywords:** 5-Deoxyadenosine salvage, 5-deoxyribose, 7-deoxysedoheptulose, 7dSh
24 biosynthesis; enzyme promiscuity, S-adenosylmethionine, radical SAM enzymes,
25 cyanobacteria

26 **Abstract**

27 7-Deoxysedoheptulose is an unusual deoxy-sugar, which acts as antimetabolite of the
28 shikimate pathway thereby exhibiting antimicrobial and herbicidal activity. It is produced by
29 the unicellular cyanobacterium *Synechococcus elongatus* PCC 7942, which has a small, stream-
30 lined genome, assumed to be free from gene clusters for secondary metabolite synthesis. In
31 this study, we identified the pathway for the synthesis of 7-deoxysedoheptulose. It originates
32 from 5-deoxyadenosine, a toxic byproduct of radical *S*-adenosylmethionine (SAM) enzymes,
33 present in all domains of life. Thereby we identified a novel 5-deoxyadenosine salvage
34 pathway, which first leads to the synthesis and excretion of 5-deoxyribose and subsequently
35 of 7-deoxysedoheptulose. Remarkably, all reaction steps are conducted by promiscuous
36 enzymes. This is a unique example for the synthesis of a bioactive compound without involving
37 a specific gene cluster. This challenges the view on bioactive molecule synthesis by extending
38 the range of possible compounds beyond the options predicted from secondary metabolite
39 gene clusters.

40 Introduction

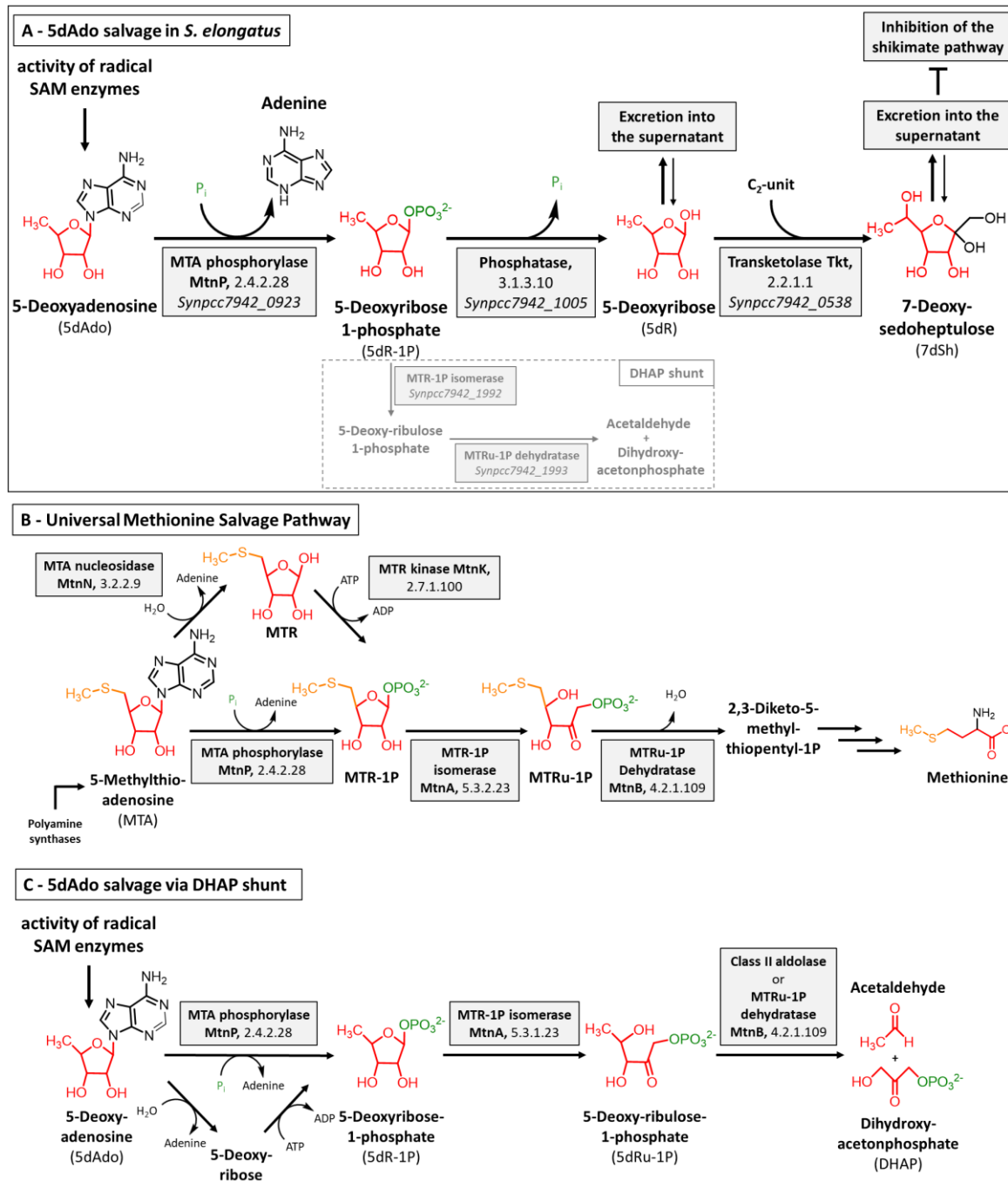
41 S-Adenosyl-L-methionine (SAM or AdoMet), which is formed by ATP and the amino acid
42 methionine, is an essential cofactor of various enzymatic reactions in all domains of life. SAM
43 can serve as a methyl group donor for the methylation of DNA, RNA and proteins in reactions
44 that release S-adenosylhomocysteine (SAH) as byproduct (**Fontecave et al., 2004**). SAM can
45 also serve as an aminopropyl donor for polyamine synthesis, and as a homoserine lactone
46 donor for the synthesis of quorum sensing compound N-acetylhomoserine lactone which both
47 result in the release of 5-methylthioadenosine (MTA). Furthermore, SAM is a source of the
48 5-deoxyadenosyl radical (5dAdo^{*}), which is formed by the activity of radical SAM enzymes
49 (**Booker and Grove, 2010; Broderick et al., 2014; Fontecave et al., 2004; Sofia et al., 2001;**
50 **Wang and Frey, 2007**). 5dAdo^{*} is formed by the reductive cleavage of SAM and can abstract
51 a hydrogen atom from its substrate to form a substrate radical as well as 5-deoxyadenosine
52 (5dAdo), which is released as a byproduct (**Marsh et al., 2010; Wang and Frey, 2007**). Radical
53 SAM enzymes, a superfamily with over 100.000 members, are present in all domains of life
54 (**Holliday et al., 2018; Sofia et al., 2001**). They are catalysing various complex chemical
55 reactions, including sulphur insertion, anaerobic oxidations, unusual methylations and ring
56 formations (**Parveen and Cornell, 2011**). Prominent members of this family are, for example,
57 involved in biotin, thiamine and lipoate biosynthesis. Other members are involved in DNA
58 repair or in the biosynthesis of secondary metabolites e.g. antibiotics (**Wang and Frey, 2007**).
59 MTA, SAH and 5dAdo are product inhibitors of these reactions (**Challand et al., 2009; Choi-**
60 **Rhee and Cronan, 2005; Farrar et al., 2010; Palmer and Downs, 2013; Parveen and Cornell,**
61 **2011**). Therefore, and because of the high bioenergetic costs of these compounds, salvage
62 pathways are necessary. SAH is rescued via the methionine cycle (**North et al., 2020**). MTA
63 salvage via the methionine salvage pathway (MSP) is also well characterised (**Sekowska and**
64 **Danchin, 2002; Wray and Abeles, 1995**) (see Figure 1 B). In the classical, aerobic MSP, MTA is
65 either processed by a two step-reaction by the MTA nucleosidase (MtnN), followed by a
66 phosphorylation by the MTR kinase (MtnK) or by the MTA phosphorylase (MtnP). The
67 subsequent reactions consist of a dehydration (MtnB, MTR-1P dehydratase), enolization and
68 phosphorylation (either by MtnC or by MtnW and MtnX), deoxygenation (MtnD) and a final
69 transamination step (MtnE) (**Sekowska et al., 2004**).

70 Despite the high abundance of radical SAM enzymes and thereby of 5dAdo, less is known
71 about 5dAdo salvage. *In vitro* experiments showed that 5dAdo can be processed by a two-step
72 reaction, in which 5dAdo is cleaved by the promiscuous MTA nucleosidase resulting in the
73 release of adenine and 5-deoxyribose (5dR) (**Challand et al., 2009; Choi-Rhee and Cronan,**
74 **2005**). The subsequent phosphorylation of 5dR by MtnK results in the formation of
75 5-deoxyribose 1-phosphate (5dR-1P). The second option is the direct conversion of 5dAdo into
76 5dR-1P and adenine via the promiscuous MTA phosphorylase (**Savarese et al., 1981**).
77 Therefore, Sekowska and coworkers suggested that 5dAdo salvage is paralogous to the MSP
78 and is driven by the promiscuous activity of the enzymes of the MSP (**Sekowska et al., 2018**).
79 Recently, a pathway for 5dR salvage was elucidated in *Bacillus thuringiensis* involving the
80 sequential activity of a kinase (DrdK), an isomerase (DrdI) and a class II aldolase (DrdA), which
81 are encoded by a specific gene cluster (**Beaudoin et al., 2018**). The authors propose that 5dR
82 is phosphorylated to 5dR-1P, which is then isomerized into 5-deoxyribulose 1-phosphate
83 (5dRu-1P) and subsequently cleaved by an aldolase into acetaldehyde and dihydroxyacetone
84 phosphate (DHAP) for primary metabolism. In organisms that lack the specific gene cluster,
85 the cleavage of 5dAdo into DHAP and acetaldehyde is proposed to occur via the promiscuous
86 activity of enzymes of the MSP. In support of this hypothesis, it was shown that
87 *Arabidopsis thaliana* DEP1, a MTR-1P dehydratase of the MSP, is promiscuous and can also
88 cleave 5dRu-1P into DHAP and acetaldehyde, suggesting that a specific aldolase is not required
89 for 5dAdo salvage (**Beaudoin et al., 2018**). In agreement with this, the promiscuous activity of
90 MSP enzymes in the 5dAdo salvage was recently reported in *Methanocaldococcus jannaschii*
91 (*M. jannaschii*) (**Miller et al., 2018**). Methylthioribose 1-phosphate isomerase (MTRI) was
92 shown to use the substrates MTR-1P, 5dR-1P and 5dR. And only recently, it was demonstrated
93 that 5dAdo is processed to DHAP and acetaldehyde by the first enzymes of the MSP and a
94 clustered class II aldolase in *Rhodospirillum rubrum* and pathogenic *Escherichia coli* strains, in
95 a process they called the “DHAP shunt” (**North et al., 2020**) (see Figure 1 C).

96 In our previous work, we isolated the rare deoxy-sugar – namely 7-deoxysedoheptulose
97 (7-deoxy-D-*altro*-2-heptulose, 7dSh) – from the supernatant of the unicellular cyanobacterium
98 *Synechococcus elongatus* PCC 7942 (henceforth referred to as *S. elongatus*) (**Brilisauer et al.,**
99 **2019**). This compound showed bioactivity towards various prototrophic organisms, e.g. other
100 cyanobacteria, especially *Anabaena variabilis* ATCC 29413 (henceforth referred to as
101 *A. variabilis*), *Saccharomyces* and *Arabidopsis*. We hypothesized that 7dSh is an inhibitor of

102 the enzyme dehydroquinate synthase (DHQS, EC 4.2.3.4) (**Brilisauer et al., 2019**), the second
103 enzyme of the shikimate pathway. Because of the streamlined genome of *S. elongatus* and
104 the lack of specific gene clusters for the synthesis of secondary metabolites (**Copeland et al.,**
105 **2014; Shih et al., 2013**) the pathway for 7dSh synthesis remained enigmatic. It is worth to
106 mention that 7dSh was also isolated from the supernatant of *Streptomyces setonensis*
107 (**Brilisauer et al., 2019; Ito et al., 1971**). Even in this species, a pathway for 7dSh biosynthesis
108 has remained unresolved. We speculated that 7dSh might be synthesized via primary
109 metabolic pathways due to enzyme promiscuity. Enzyme promiscuity, the ability of an enzyme
110 to use various substrates, is especially important for organisms with a small genome.
111 Previously it was described that the marine cyanobacterium *Prochlorococcus* uses a single
112 promiscuous enzyme that can transform up to 29 different ribosomally synthesized peptides
113 into an arsenal of polycyclic bioactive products (**Li et al., 2010**). As from the 7dSh-containing
114 supernatant of *S. elongatus* we additionally isolated the deoxy-sugar 5-deoxy-D-ribose (5dR),
115 we hypothesized that 5dR could serve as a putative precursor molecule of 7dSh (**Brilisauer et**
116 **al., 2019**). *In vitro*, 5dR can serve as a substrate for a transketolase-based reaction, in which a
117 C₂-unit (e.g. from hydroxypyruvate) is transferred to the C₅-unit (3*S*, 4*R* configured) leading
118 to the formation of 7dSh (**Brilisauer et al., 2019**).

119 In this work we identified the pathway for 7dSh biosynthesis, which involves a new salvage
120 route for 5dAdo resulting in the release of 5dR and 7dSh in the culture medium. Therefore,
121 *S. elongatus* can synthesize an allelopathic inhibitor from the products of the primary
122 metabolism by using promiscuous enzymes.



123

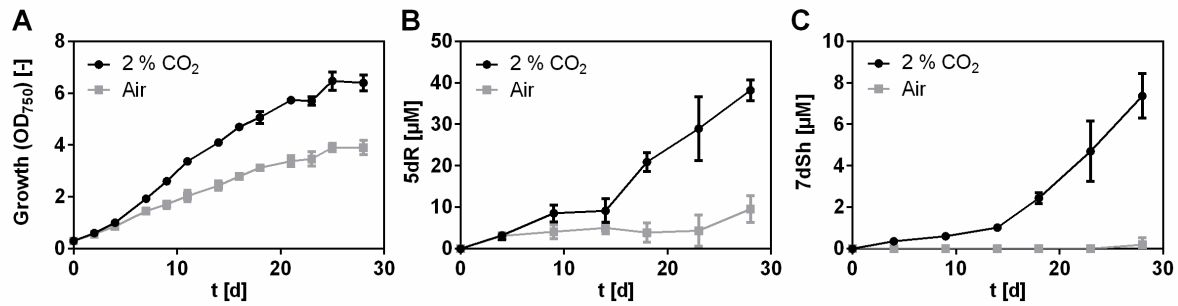
124 **Figure 1: Overview of the 5dAdo and MTA salvage pathways.** (A) - 5dAdo salvage in
 125 *Synechococcus elongatus* via the excretion of the bioactive deoxy-sugars 5dR and 7dSh (this
 126 study). 5dR-1P is partially also metabolized via the DHAP shunt (shown by dashed line),
 127 especially under low carbon conditions. (B) - Universal methionine salvage pathway (MSP)
 128 (*Sekowska et al., 2004*). MTR: Methylthioribose, MTRu-1P: Methylthioribulose-1P, (C) - 5dAdo
 129 salvage via the DHAP shunt (*Beaudoin et al., 2018; North et al., 2020*).

130 **Results**

131 **5dR and 7dSh accumulation in supernatants of *S. elongatus* is strongly promoted by CO₂** 132 **supplementation**

133 Previously we estimated the content of 7dSh in the supernatant of *S. elongatus* cultures via a
134 bioassay based on the size of the inhibition zone of *A. variabilis* exposed to the supernatant
135 of *S. elongatus* (**Brilisauer et al., 2019**). The content of 5dR was neither estimated nor
136 quantified before. To decipher the biosynthesis of 5dR and 7dSh in *S. elongatus*, we developed
137 a gas chromatography-mass spectrometry (GC-MS)-based method that enables the detection
138 and absolute quantification of low μM concentrations of these metabolites in the supernatant
139 of cyanobacterial cultures (see Material and Methods). Briefly, 200 μL of culture supernatant
140 were lyophilized and extracted with chloroform, methanol, and H₂O. Subsequently, the polar
141 phase was chemically derivatised with methoxylamine and MSTFA for GC-MS analysis. As
142 already reported (**Brilisauer et al., 2019**), 7dSh accumulation in the supernatant requires
143 elevated CO₂ supply to the cultures (Figure 2 C). Under 2 % CO₂ supplementation, 5dR
144 gradually accumulated with increasing optical density of the cultures, whereas 7dSh
145 accumulation only started during a later growth phase. After 30 days of growth, the amount
146 of 7dSh in the supernatant was around one quarter compared to that of 5dR. 5dR
147 accumulation was strongly promoted by CO₂ supplementation, however, a small amount
148 already started to accumulate in the cultures under ambient air conditions (Figure 2 B).

149 Although the optical density of the aerated cultures in the last days of the experiment reached
150 values that were similar to those of the CO₂-supplemented cultures, where 7dSh accumulation
151 started, 7dSh could never be detected in air-grown cultures. This suggests that the formation
152 of the deoxy-sugars is not only dependent on a certain cell density, but is also related to a
153 specific metabolic state.

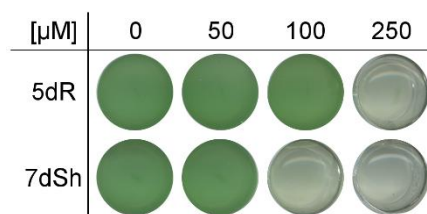


154

155 **Figure 2: 5dR and 7dSh accumulation in the supernatant of *S. elongatus* is strongly promoted**
 156 **by high CO₂ concentrations.** *S. elongatus* cultures aerated either with ambient air (grey

157 squares) or with air supplemented with 2 % CO₂ (black dots). (A) Over time growth of
 158 *S. elongatus* (indicated by OD₇₅₀). Over time concentration of 5dR (B) or 7dSh (C) in the
 159 supernatant of *S. elongatus* cultures. Note the different values of the y-axis. Data shown
 160 represent mean and standard deviation of three independent biological replicates.

161 To gain further insights into 5dR/7dSh metabolism, we measured the intracellular
 162 concentration of 5dR and 7dSh over the whole cultivation process but were hardly able to
 163 detect any of either deoxy-sugar (Figure S1). Moreover, the small intracellular amount
 164 remained nearly constant while the extracellular concentration increased. The fact that 5dR
 165 and 7dSh only accumulate in the supernatant but is almost undetectable intracellularly
 166 strongly suggests that extracellular 5dR/7dSh accumulation is not due to cell lysis but due to
 167 secretion of the compounds immediately after their formation. Removal of these metabolites
 168 from the cytoplasm is probably essential for *S. elongatus* as both molecules showed growth
 169 inhibition towards the producer strain at elevated concentrations (Figure 3). 7dSh is
 170 bactericidal at concentrations of 100 µM, while 5dR is bacteriostatic at concentrations of
 171 250 µM.

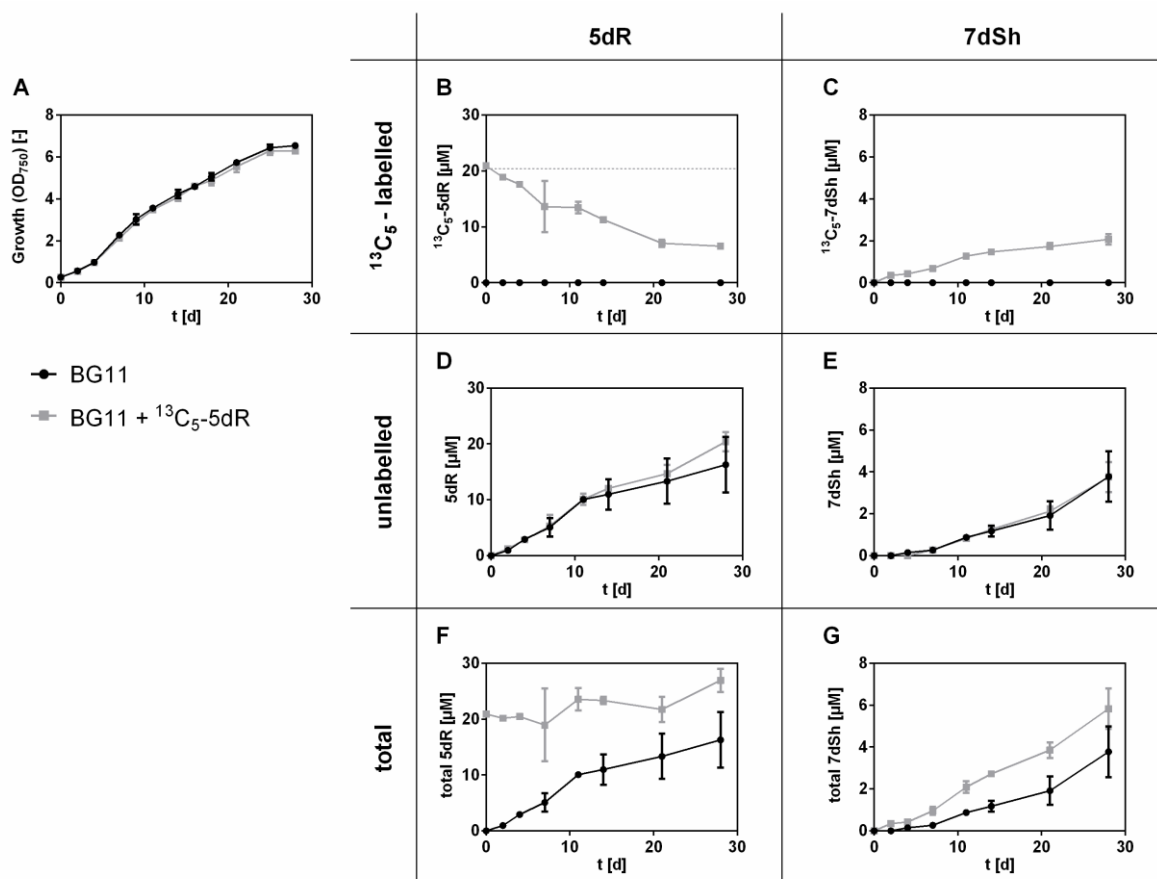


172

173 **Figure 3: 5dR and 7dSh are inhibiting the growth of the producer strain.** Effect of different
 174 concentrations of 5dR and 7dSh on the growth of *S. elongatus*. The cultures were inoculated
 175 at OD₇₅₀ = 0.1 in 1 mL BG11 medium in the absence (0) or presence of either 5dR or 7dSh at
 176 the indicated concentrations and grown in a 24-well plate for 3 days. The experiment was
 177 performed in triplicates. The results of one replicate are shown.

178 **5dR is a precursor molecule for 7dSh biosynthesis *in vivo***

179 In our previous work, we reported the *in vitro* synthesis of 7dSh by converting 5dR into 7dSh
 180 by a transketolase-based reaction with hydroxypyruvate as a C₂-unit donor (*Brilisauer et al.,*
 181 **2019**). To determine whether 5dR might also be a precursor molecule for 7dSh *in vivo*, a 5dR-
 182 feeding experiment was performed (Figure 4). To unambiguously distinguish the naturally
 183 formed and the supplemented 5dR, uniformly labelled [U-¹³C₅]-5dR (¹³C₅-5dR) was
 184 synthesized and added at a final concentration of 20 μM to *S. elongatus* cultures at the
 185 beginning of the cultivation. The concentration of labelled (Figure 4 B, C), unlabelled
 186 (Figure 4 D, E) and the total amount of 5dR and 7dSh (Figure 4 F, G) was determined by GC-MS
 187 at different time points over a period of 30 days.



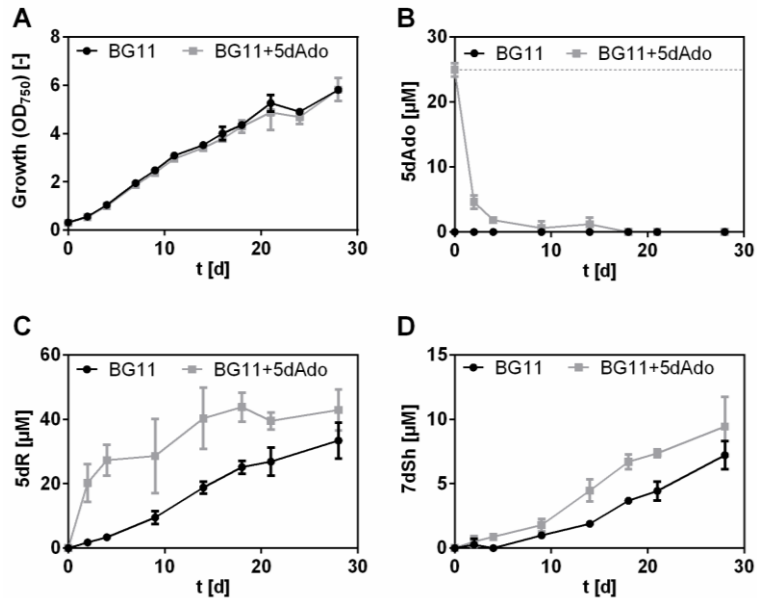
188
 189 **Figure 4: 5dR is the precursor molecule of 7dSh.** Effects of ¹³C₅-5dR supplementation over the
 190 time on the growth of *S. elongatus* (A) or on the concentration of ¹³C₅-5dR (B), ¹³C₅-7dSh (C),
 191 unlabelled 5dR (D), unlabelled 7dSh (E), total 5dR (F) and total 7dSh (G) in the culture
 192 supernatant. 20 μM ¹³C₅-5dR (indicated by dashed line) was added at the beginning of the
 193 cultivation (grey squares). Control cultures (black dots) were cultivated in BG11 without
 194 supplemented ¹³C₅-5dR. All cultures were aerated with air supplemented with 2 % CO₂. Values
 195 shown in the graphs represent mean and standard deviation of three biological replicates.

196 Neither the growth of *S. elongatus* nor the excretion of unlabelled, intracellular synthesized
197 5dR and 7dSh was affected by the addition of exogenous $^{13}\text{C}_5$ -5dR (Figure 4 A, D, E). We found
198 that $^{13}\text{C}_5$ -5dR is taken up by the cultures as its concentration in the supernatant continuously
199 decreased (Figure 4 B, grey squares). Already within 2 days, $^{13}\text{C}_5$ -7dSh could be detected in the
200 supernatant of these cultures (Figure 4 C, grey squares), clearly proving that $^{13}\text{C}_5$ -7dSh was
201 formed from the precursor molecule $^{13}\text{C}_5$ -5dR. However, only a small amount of exogenously
202 added $^{13}\text{C}_5$ -5dR was converted into 7dSh. At the end of the experiment, 10 % of the initially
203 applied $^{13}\text{C}_5$ -5dR (20 μM) was converted into $^{13}\text{C}_5$ -7dSh (around 2 μM). Around 30 % of
204 $^{13}\text{C}_5$ -5dR remained in the supernatant (6.5 μM). The residual amount is assumed to be
205 metabolised via (an)other pathway(s). Because unlabelled 5dR was excreted at the same time
206 as $^{13}\text{C}_5$ -5dR was taken up (Figure 4 B, D), we conclude that 5dR must be imported and exported
207 in parallel.

208

209 **5dAdo as a precursor molecule of 7dSh**

210 Next, we asked the question where 5dR is derived from and this drew our attention to 5dAdo,
211 a byproduct of radical SAM enzymes (**Wang and Frey, 2007**). The compound has to be
212 removed because of its intracellular toxicity (**Choi-Rhee and Cronan, 2005**), and its cleavage
213 can result in the formation of 5dR (**Beaudoin et al., 2018; Choi-Rhee and Cronan, 2005**) (see
214 Figure 1 C). To prove the hypothesis that 7dSh is formed as a result of 5dAdo salvage in
215 *S. elongatus*, 5dAdo feeding experiments were performed and the supernatants were
216 analysed by GC-MS (Figure 5). Notably, the growth of *S. elongatus* was not affected by
217 supplementation with 5dAdo, which was taken up very quickly (Figure 5 A, B). After 4 days,
218 almost all 5dAdo was taken up. A control experiment showed that the rapid decline in the
219 amount of 5dAdo in the supernatant was not caused by the instability of 5dAdo in the
220 medium. Feeding of the cells with 5dAdo immediately led to an enhanced accumulation of
221 5dR in the culture supernatant (Figure 5 C). After 14 days, 7dSh accumulation in 5dAdo-
222 supplemented cultures was clearly enhanced in comparison to control cultures (Figure 5 D),
223 supporting our hypothesis that 5dAdo is a precursor molecule of 7dSh. This experiment also
224 revealed that only about half of the supplemented 5dAdo (initial concentration: 25 μM) is
225 converted into 5dR and 7dSh, because at the end of the growth experiment the 5dR content
226 in the supplemented cultures is increased by around 10 μM , and that of 7dSh by 2 μM . This
227 suggest that other pathway(s) for 5dAdo salvage must exist.

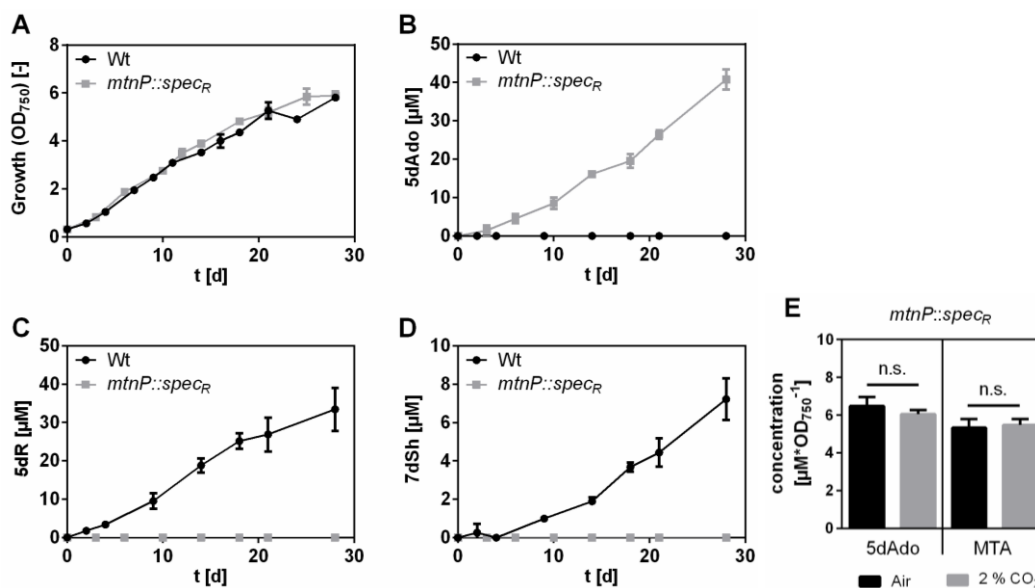


228

229 **Figure 5: 5dAdo feeding experiment.** Effect of 5dAdo-supplementation on the growth of
230 *S. elongatus* (A) or on the concentration of 5dAdo (B), 5dR (C) and 7dSh (D) in the culture
231 supernatant. 25 μM 5dAdo (indicated by dashed line) was added at the beginning of the
232 cultivation (grey squares). Control cultures (black dots) were cultivated in BG11 in absence of
233 exogenous 5dAdo. All cultures were aerated with air supplemented with 2 % CO₂. Note the
234 different values of the y-axis. Values shown in the graphs represent mean and standard
235 deviation of three biological replicates.

236 5dAdo is known to be cleaved either by the MTA nucleosidase (MtnN) or by the MTA
237 phosphorylase (MtnP) (*Challand et al., 2009; Choi-Rhee and Cronan, 2005; Savarese et al.,*
238 *1981*). The first reaction leads to the release of adenine and 5dR, the latter is phosphate-
239 dependent and leads to the release of adenine and 5dR-1P. In *S. elongatus*, no homologous
240 gene for a MTA nucleosidase was found, but gene *Synpcc7942_0923* is annotated as a MTA
241 phosphorylase. Therefore, an insertion mutant of *Synpcc7942_0923* was generated via the
242 replacement of the gene by an antibiotic resistance cassette (*S. elongatus mtnP::specR*). Under
243 conditions favourable for 5dR/7dSh production the mutant grew like the wild type
244 (Figure 6 A). A GC-MS analysis of the culture supernatant revealed that the mutant neither
245 excreted 5dR nor 7dSh (Figure 6 C, D). Instead, while undetectable in the supernatant of the
246 wild type strain, 5dAdo strongly accumulated in the supernatant of *S. elongatus mtnP::specR*
247 cultures (Figure 6 B). This clearly showed that 5dR/7dSh are derived from 5dAdo in an MtnP
248 dependent manner. Due to the detoxification via excretion, the *mtnP::specR* mutant escapes
249 the toxic effect of 5dAdo and does not show any growth disadvantage (Figure 6 A). It has
250 previously been reported that a *mtnP* knockout mutant in *S. cerevisiae* as well as MtnP-
251 deficient mammalian tumour cells excreted MTA (*Chattopadhyay et al., 2006; Kamatani and*

252 **Carson, 1980**). Both MTA and 5dAdo are known to be cleaved by MtnP (**Savarese et al., 1981**).
253 Consistently, the *mtnP::spec_R* mutant excretes MTA as well as 5dAdo (Figure 6 E). As 5dR/7dSh
254 formation is strongly dependent on the cultivation at elevated CO₂ concentration we
255 measured the amount of 5dAdo and MTA in cultures of the *mtnP::spec_R* mutant supplied with
256 ambient air or with air enriched with 2 % CO₂. It turned out that the amounts of excreted
257 5dAdo and MTA (normalized to the optical density of the cultures) are almost identical under
258 atmospheric or elevated CO₂ conditions (Figure 6 E). This clearly indicates that 5dAdo salvage
259 via 5dR/7dSh formation and excretion at high CO₂ conditions is not triggered by an increased
260 synthesis of the precursor molecule 5dAdo compared to ambient CO₂ concentrations. Rather,
261 it appears that 5dAdo is actively metabolised into 5dR/7dSh under elevated CO₂ conditions,
262 whereas 5dAdo salvage under ambient CO₂ conditions is conducted by (an)other pathway(s).
263 Since the MTA formation is also unaltered (Figure 6 E), we exclude that 5dAdo salvage via
264 5dR/7dSh formation is triggered by an enhanced demand of MTA salvage via a bifunctional
265 MTA/5dAdo salvage pathway.



266

267 **Figure 6: 5dAdo is cleaved by MtnP and then metabolised into 5dR and 7dSh in *S. elongatus***
268 **at high CO₂ concentrations.** Growth (A), concentrations of 5dAdo (B), 5dR (C) and 7dSh (D) in
269 the supernatant of *S. elongatus* wild type (black dots) or *mtnP::spec_R* mutant (grey squares).
270 All cultures were aerated with air supplemented with 2 %CO₂. Note the different values of the
271 y-axis. (E) 5dAdo and MTA concentrations in the supernatant of the *mtnP::spec_R* mutant
272 normalised on the optical density after 11 days of cultivation (cultures were either aerated
273 with atmospheric air (black) or with air supplemented with 2 % CO₂ (grey)). Values shown in
274 the graphs represent mean and standard deviation of three biological replicates.

275 **5dR and 7dSh formation is not ubiquitous**

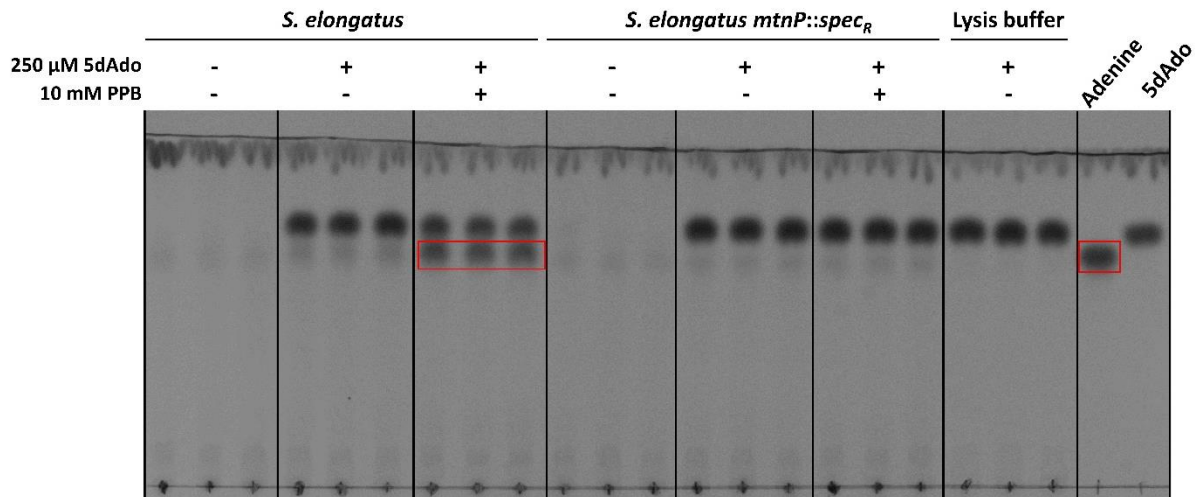
276 To clarify how widespread the synthesis of 7dSh or 5dR is in cyanobacteria, we analysed the
277 supernatants of other cyanobacterial strains via GC-MS (*Synechococcus* sp. PCC 6301,
278 *Synechococcus* sp. PCC 7002, *Synechococcus* sp. PCC 6312, *Synechococcus* sp. PCC 7502,
279 *Synechocystis* sp. PCC 6803, *Anabaena variabilis* ATCC 29413, *Nostoc punctiforme*
280 ATCC 29133, *Anabaena* sp. PCC 7120). Only in three of five *Synechococcus* strains, the
281 deoxy-sugars 5dR and 7dSh were detectable in the supernatant. All the other strains
282 accumulated neither 5dR nor 7dSh. In the freshwater strain *Synechococcus* sp. PCC 6301, the
283 amounts of 7dSh and 5dR were in a similar concentration range to those in *S. elongatus*. This
284 is not surprising since the genome of *Synechococcus* sp. PCC 6301 is nearly identical to that of
285 *S. elongatus* PCC 7942 (**Sugita et al., 2007**). Very small amounts of 5dR and 7dSh were
286 detected in the marine strain *Synechococcus* sp. PCC 7002. In *Streptomyces setonensis*, which
287 was shown to produce 7dSh (**Brilisauer et al., 2019; Ito et al., 1971**), we detected $113 \pm 7 \mu\text{M}$
288 7dSh but no 5dR in the supernatant of cultures grown for 7 days.

289

290 **5dAdo cleavage is strictly dependent on phosphorylase activity**

291 To further characterize the cleavage of 5dAdo in *S. elongatus*, a crude extract assay was
292 performed. Crude extracts of *S. elongatus* wild type and *mtnP::spec_R* mutant cells were
293 incubated with 5dAdo in the presence or absence of potassium phosphate buffer (PPB).
294 Analysis of the extracts via thin layer chromatography revealed that 5dAdo cleavage and,
295 thereby, adenine release is strictly dependent on the presence of phosphate (Figure 7).
296 Adenine is only released by *S. elongatus* cell extracts in the presence of potassium phosphate
297 buffer (red label), but not by *mtnP::spec_R* mutant cells, which are not capable of 5dAdo
298 cleavage. Therefore, 5dAdo cleavage in *S. elongatus* is strictly dependent on the presence of
299 the MTA phosphorylase. Other enzymes, for example purine nucleosidase phosphorylases
300 (**Lee et al., 2004**), apparently do not process 5dAdo in the *S. elongatus* cell extract. This result
301 implies that the first product of 5dAdo cleavage must be 5dR-1P, which is subsequently
302 converted into 5dR. 5dR-1P seemed quite stable because liquid chromatography (LC)-MS
303 analysis revealed that a compound with a *m/z* ratio that corresponds to the sum formula of
304 5dR-1P ($[\text{M}+\text{H}, \text{M}+\text{Na}]^+$ (*m/z* 215.0315; 237.0135)) accumulated in the crude extract
305 (Figure S2). Furthermore, no 5dR formation was observed in the crude extracts (Figure S3).

306 With this, we exclude a spontaneous hydrolysis of 5dR-1P which is in accordance to the
307 literature, where 5dR-1P is reported to be metabolically stable (*Plagemann and Wohlhueter,*
308 **1983**).



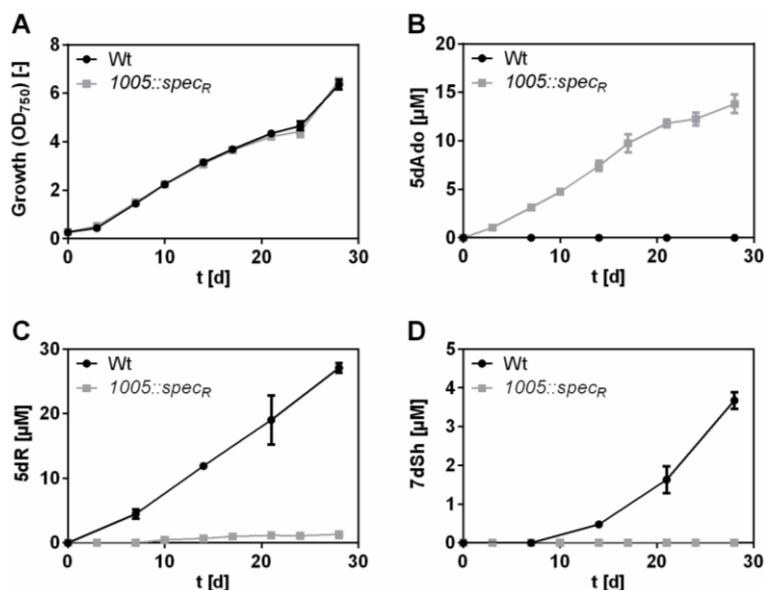
309
310 **Figure 7: 5dAdo cleavage in *S. elongatus* is phosphate dependent.** Crude extracts from
311 *S. elongatus* or *S. elongatus mtnP::spec_R* were incubated with 5dAdo in the presence or
312 absence of potassium phosphate buffer (PPB) and then analysed via thin layer
313 chromatography on silica gel. 5dAdo ($R_f=0.68$) and adenine ($R_f=0.76$) analytes were visualized
314 via absorption at 254 nm. Pure adenine and 5dAdo were used as standards (right). Spots
315 corresponding to adenine are highlighted with a red box. Three independent replicates are
316 shown for each condition. The stability of 5dAdo in the buffer is shown with the lysis buffer
317 control.

318

319 **5dR-1P is dephosphorylated by a specific phosphatase**

320 As 5dR-1P is metabolically stable we assumed the involvement of a specific phosphatase in
321 5dR-1P dephosphorylation. The dephosphorylation of 5dR-1P in 5dAdo salvage is surprising as
322 in the literature it is suggested that the phosphorylation of 5dR is essential for its further
323 metabolization (*Beaudoin et al., 2018; North et al., 2020; Sekowska et al., 2018*). To identify
324 the responsible phosphatase, we analysed the genome of *S. elongatus* regarding the presence
325 of phosphoric monoester hydrolases (see Table S3, Supporting information).
326 *Synpcc7942_1005*, which is annotated as glucose-1-phosphatase, belonging to the haloacid
327 dehalogenase (HAD)-like hydrolase superfamily subfamily IA (*Burroughs et al., 2006; Koonin*
328 **and Tatusov, 1994**), seemed a promising candidate as only *S. elongatus* and *Synechococcus* sp.
329 PCC 6301, which both produce larger amounts of 5dR/7dSh, possess a homologous gene. The
330 other cyanobacteria mentioned above do not possess it. Furthermore, phosphatases from the

331 HAD-like hydrolase superfamily are known to be promiscuous enzymes dephosphorylating
332 various phosphate-sugars (*Kuznetsova et al., 2006; Pradel and Boquet, 1988*). To examine
333 whether this gene is essential for 5dR-1P dephosphorylation or 5dR/7dSh synthesis, an
334 insertion mutant of this gene was created by the replacement with a spectinomycin resistance
335 cassette (*S. elongatus Synpcc7942_1005::spec_R*). Under 5dR/7dSh production conditions (air
336 supplemented with 2 % CO₂) the mutant grew like the wildtype (Figure 8 A). Whereas the
337 wildtype excretes 5dR and 7dSh, the mutant only excretes minor amounts of 5dR and no 7dSh
338 (Figure 8 C, D). Instead, the mutant excreted 5dAdo, which was never detected in the
339 supernatant of the wildtype (Figure 8 B). This clearly shows that the gene product of
340 *Synpcc7942_1005* is the major enzyme for the dephosphorylation of 5dR-1P. However, since
341 even in the mutant small quantities of 5dR were detectable, we suggest that in addition to the
342 gene product of *Synpcc7942_1005* other phosphatases may contribute to residual 5dR-1P
343 dephosphorylation. In agreement with this conclusion, we found that *Synechococcus* sp.
344 PCC 7002, which does not possess a homolog of *Synpcc7942_1005* also excreted minor
345 amounts of 5dR and 7dSh (see above).



346
347 **Figure 8: 5dR-1P is dephosphorylated by a phosphatase from the HAD hydrolase superfamily**
348 **(*Synpcc7942_1005*, EC 3.1.3.10).** Growth (A), concentrations of 5dAdo (B), 5dR (C) and 7dSh
349 (D) in the supernatant of *S. elongatus* wild type (black dots) or *1005::spec_R* mutant (grey
350 squares). All cultures were aerated with air supplemented with 2 %CO₂. Note the different
351 values of the y-axis. Values shown in the graphs represent mean and standard deviation of
352 three biological replicates.

353 **5dR/7dSh producers possess complete MSP gene clusters**

354 By analysing the genomes of all examined cyanobacteria in this study, it turned out that those
355 strains that do not produce 5dR and 7dSh only possess annotated genes for the first two
356 reactions of the MSP (*mtnP* and *mtnA*), whereas the producer strains possess annotated genes
357 for the whole MSP pathway (Table S1). The 5dAdo salvage via the DHAP shunt requires a
358 specific class II aldolase, e.g. *DrdA* in *B. thuringiensis* (**Beaudoin et al., 2018**) or *Ald2* in
359 *R. rubrum* (**North et al., 2020**), which is clustered with the first enzymes of the MSP, e.g. *MtnP*
360 or *MtnN/MtnK* and *MtnA* in *R. rubrum*) or with a specific phosphorylase and isomerase as
361 shown for *B. thuringiensis*. *In vitro* data suggest that the MTRu-1P-dehydratase (*MtnB*) from
362 the MSP can also act as a promiscuous aldolase thereby completing the 5dAdo salvage via the
363 DHAP shunt (**Beaudoin et al., 2018; North et al., 2020**). Since none of the analysed strains
364 possesses such an *Ald2* homolog, we assume that 5dR/7dSh producing strains might use the
365 DHAP shunt by using *MtnB* under certain conditions. The 5dR/7dSh non-producer strains must
366 employ another pathway of 5dAdo salvage or use another aldolase for the DHAP shunt.

367 Discussion

368 Radical SAM enzymes are important enzymes in all domains of life (*Sofia et al., 2001*). A
369 byproduct of the activity of these enzymes is 5dAdo (*Wang and Frey, 2007*). Its accumulation
370 inhibits the activity of the radical SAM enzymes themselves (*Challand et al., 2009; Choi-Rhee*
371 *and Cronan, 2005; Farrar et al., 2010; Palmer and Downs, 2013*). Therefore, 5dAdo salvage
372 pathways are essential. In this study we showed that the unicellular cyanobacterium
373 *S. elongatus* PCC 7942 has a special salvage route for 5dAdo, which was never reported before
374 (Figure 1 A). We show that 5dAdo salvage can be achieved by the excretion of 5-deoxyribose
375 and 7-deoxysedoheptulose. 5dR as a product of 5dAdo cleavage was postulated (*Parveen and*
376 *Cornell, 2011; Sekowska et al., 2018*) or observed before but only in *in vitro* assays (*Choi-Rhee*
377 *and Cronan, 2005; Sekowska et al., 2018*). Beaudoin and coworkers suggested 5dR excretion
378 as a detoxification strategy for organisms that do not possess a specific gene cluster for 5dAdo
379 salvage (*Beaudoin et al., 2018*) (analogous to MTR excretion in *E. coli* which does not possess
380 a complete MSP (*Hughes, 2006; Schroeder et al., 1972*)). Therefore, 5dR accumulation in the
381 supernatant of *S. elongatus* as an *in vivo* phenomenon was first reported by our previous
382 publication (*Brilisauer et al., 2019*), and here identified as a result of 5dAdo salvage.

383 We propose the following model for a possible 5dAdo salvage route in *S. elongatus* by the
384 activity of promiscuous enzymes leading to the synthesis of the bioactive deoxy-sugars 5dR
385 and 7dSh (Figure 1 A). In brief, 5dAdo is processed by the promiscuous MTA phosphorylase
386 into 5dR-1P. Under elevated CO₂ conditions, this molecule is dephosphorylated to 5dR by a
387 potentially promiscuous phosphatase to 5dR, part of which is excreted and part of which is
388 further metabolized by the activity of a promiscuous transketolase to 7dSh, which is also
389 excreted from the cells to avoid its inhibitory effects on the shikimate pathway (*Brilisauer et*
390 *al., 2019*). 7dSh is a potent inhibitor of the dehydroquinate synthase, but the inhibitory effect
391 of the compound is dependent on the organism. The producer strain tolerates high
392 concentrations of 7dSh (Figure 3), whereas f.e. *A. variabilis* is highly sensitive towards 7dSh
393 treatment (*Brilisauer et al., 2019*), suggesting that 7dSh is a potent allelopathic inhibitor.

394 Although most bacteria possess the enzymes for a two-step reaction of 5dAdo cleavage (MTA
395 nucleoside and MTR kinase) (*Albers, 2009; Zappia et al., 1988*), all examined cyanobacteria
396 possess a MTA phosphorylase (MtnP) (Table S1), which is normally present in eukaryotes
397 (except for plants). The phenotype of the insertion mutant (*mtnP::specR*), which excretes

398 5dAdo instead of 5dR/7dSh, demonstrates that 5dR and 7dSh are products of 5dAdo salvage
399 (Figure 6). The 5dAdo salvage routes previously reported suggest that the phosphorylation of
400 5dR or the 5dR moiety of 5dAdo is essential to further metabolise the molecules via specific
401 enzymes or by promiscuous activity of the enzymes of the MSP (**Beaudoin et al., 2018; North**
402 **et al., 2020; Sekowska et al., 2018**). In *S. elongatus* however, 5dR-1P is subsequently
403 dephosphorylated to 5dR for excretion or for further processing to 7dSh. Our data imply that
404 the dephosphorylation of 5dR-1P is not due to spontaneous hydrolysis but is mainly conducted
405 by the gene product of *Synpcc7942_1005* (see Figure 8). *Synpcc7942_1005* belongs to Mg²⁺-
406 dependent class IA HAD-like hydrolase superfamily (**Burroughs et al., 2006**) and is annotated
407 as a glucose-1-phosphatase, which catalyses the dephosphorylation of glucose 1-phosphate
408 (**Turner and Turner, 1960**). As these phosphatases can also exhibit phytase activity (**Herter et**
409 **al., 2006; Suleimanova et al., 2015**) we assume that the gene product of *Synpcc7942_1005*
410 might also exhibits promiscuous activity, including 5dR-1P dephosphorylation. The
411 dephosphorylation of a similar molecule (5-fluoro-5-deoxyribose 1-phosphate) by a specific
412 phosphoesterase (FdrA) is also conducted by *Streptomyces* sp. MA37 during the production of
413 a specific secondary fluorometabolite (**Ma et al., 2015**) (pathway shown in Figure S4).

414 In later growth phases, small amounts of 5dR are transformed into 7dSh which is then also
415 immediately excreted into the supernatant (Figure 2 C, Figure 4 C, E). In our previous work we
416 showed that the affinity of *S. elongatus* transketolase for 5dR ($k_m=108.3$ mM) is 100-fold lower
417 than for the natural substrate D-ribose-5-phosphate ($k_m=0.75$ mM) (**Brilisauer et al., 2019**).
418 This is in accordance with the fact that 7dSh is only formed when relatively high extracellular
419 5dR concentrations are reached (either in later growth phases or due to the addition of
420 externally added 5dR; note that 5dR is continuously imported and exported). Furthermore,
421 only one tenth of ¹³C₅-5dR is converted into ¹³C₅-7dSh. 7dSh formation from 5dR is therefore
422 an impressive example how a more potent “derivative” (7dSh) is formed by promiscuous
423 enzyme activity. Interestingly, a promiscuous transketolase reaction was also suggested in
424 later steps of anaerobic 5dAdo salvage in *M. jannaschii*, in which 5dRu-1P is cleaved into
425 lactaldehyde and methylglyoxal (**Miller et al., 2018**). *Streptomyces setonensis* (not yet
426 sequenced) accumulates much higher concentrations of 7dSh in the supernatant than
427 *S. elongatus* but no 5dR at all, which supports the hypothesis that 7dSh might be derived from
428 complete conversion of 5dR by a more specific transketolase.

429 In high concentrations, 5dR exhibited toxicity towards the producer strain (Figure 3). 5dR
430 toxicity was also reported in *B. thuringiensis* (**Beaudoin et al., 2018**), but the intracellular
431 target is not yet known. Therefore, *S. elongatus* has to steadily excrete 5dR into the
432 supernatant to avoid intracellular toxicity. Because $^{13}\text{C}_5$ -5dR is taken up at the same time as
433 unlabelled 5dR is excreted (Figure 4 B, D), it is obvious that 5dR is continuously imported and
434 exported so that hardly any 5dR accumulates intracellularly (see Figure S1). We also assume
435 that 7dSh is im- and exported, too. This suggests the presence of an effective export system
436 which is essential for the survival of the producer strain.

437 5dAdo salvage via 5dR and 7dSh excretion was only observed when cultures were aerated
438 with air supplemented with 2 % CO_2 (Figure 2 B, C). Since equal amounts of 5dAdo were
439 formed under ambient CO_2 as under high CO_2 conditions (Figure 6 E), we assumed that under
440 ambient CO_2 conditions 5dAdo salvage is conducted via (an)other pathway(s). The occurrence
441 of (an) additional 5dAdo salvage pathway(s) in *S. elongatus* is underlined by the fact that
442 5dAdo is not completely metabolised into 5dR/7dSh even under high CO_2 conditions
443 (Figure 5). Because *S. elongatus* and the other 5dR/7dSh producers are equipped with the
444 enzymes for the whole MSP (see Table S1), we hypothesize that 5dAdo can be also
445 metabolised via promiscuous activity of the enzymes of the MSP via the “DHAP-shunt”
446 resulting in the formation of DHAP and acetaldehyde (see Figure 1 A, C) as suggested for
447 organisms that do not possess a specific gene cluster for 5dAdo salvage (**Beaudoin et al., 2018**;
448 **North et al., 2020**; **Sekowska et al., 2018**). The formation of MTA, the starting molecule of the
449 MSP, is almost identical under atmospheric and high carbon conditions (Figure 6 E). This
450 indicates that 5dAdo salvage via 5dR/7dSh excretion under high CO_2 conditions is not
451 triggered by an increased demand of MTA salvage. It is known that intracellular $\text{CO}_2/\text{HCO}_3^-$ (C_i)
452 exhibits regulatory functions at the metabolic and transcriptomic level (**Blombach and Takors,**
453 **2015**): $\text{CO}_2/\text{HCO}_3^-$ can alter physiochemical enzyme properties and it is known to regulate
454 virulence and toxin production in pathogens, e.g. in *Vibrio cholerae* (**Abuaita and Withey,**
455 **2009**). In particular, cyanobacteria strongly respond to the ambient C_i supply by a multitude
456 of metabolic adaptations such as carbon concentrating mechanisms (**Burnap et al., 2015**) and
457 the synthesis of cAMP (**Selim et al., 2018**). As we hypothesize that the fate of 5dAdo is a
458 regulated process, we assume that the dephosphorylation of 5dR and the subsequent
459 formation of 7dSh molecules is not an “accident”. They are rather purposely formed

460 metabolites, which however derive from toxic byproducts of the primary metabolism. The
461 regulation how 5dAdo is directed towards 5dR/7dSh formation has to be further investigated.

462 With 18 radical SAM enzymes (see Table S2), *S. elongatus* only possesses a relatively small
463 number of radical SAM enzymes compared to other prokaryotes (*B. thuringiensis*: 15; other
464 Firmicutes: more than 40 (**Beaudoin et al., 2018**), *R. rubrum*: 25, *M. jannaschii*: 30 (**North et**
465 **al., 2020**)). Probably the most important radical SAM enzymes under the cultivation
466 conditions applied here are involved in cofactor biosynthesis: Lipoic acid synthase (LipA),
467 biotin synthase (BioB) and GTP 3',8-cyclase (MoaA), which is involved in molybdopterin
468 biosynthesis. These cofactors are presumably equally important under atmospheric or high
469 carbon conditions resulting in the unaltered 5dAdo formation, thereby explaining the
470 unaltered rate of 5dAdo formation.

471 7dSh can inhibit the growth of other cyanobacteria but also of plants, and was therefore
472 suggested to be an allelopathic inhibitor by inhibiting the dehydroquinate synthase, the
473 second enzyme of the shikimate pathway (**Brilisauer et al., 2019**). Additionally, 5dR is toxic for
474 various organisms (Figure 3, (**Beaudoin et al., 2018**)). Despite the low concentrations of
475 5dR/7dSh observed under laboratory conditions it is imaginable that excretion of 5dR and
476 7dSh plays a role in protecting the ecological niche of the producer strains. 7dSh is a more
477 potent inhibitor for example for *A. variabilis* than for the producer strain. A bactericidal effect
478 for *A. variabilis* was observed at concentrations of 13 μ M 7dSh (**Brilisauer et al., 2019**),
479 whereas *S. elongatus* is affected by 100 μ M (see Figure 3). In its natural environment,
480 *S. elongatus* is able to form biofilms (**Golden, 2019; Yang et al., 2018**). In biofilms
481 cyanobacteria tend to excrete exopolysaccharides (**Rossi and Philippis, 2015**) which can be
482 used as a carbon source by heterotrophic members of the microbial community thereby
483 causing locally elevated CO₂ concentrations. This could lead to a local enrichment of 5dR and
484 7dSh, thereby providing a growth advantage to the producer strains protecting their niches
485 against competing microalgae.

486

487 **Conclusion**

488 5dAdo salvage is a less noticeable and overlooked research topic in comparison to methionine
489 salvage from MTA. Hence, it should be further investigated above all because 5dAdo is present
490 in all domains of life whereas MTA is only produced by specific organisms. It is possible that

491 additional metabolites, apart from 7dSh, are derived from 5dAdo salvage in other organisms.
492 This study shows that enzyme promiscuity is especially important for organisms with a small
493 genome, since it enables them to produce special metabolites in absence of *ad hoc*
494 biosynthetic gene clusters.

495 **Materials and Methods**

496 **Cultivation**

497 *Synechococcus elongatus* PCC 7942 was cultivated under photoautotrophic conditions in
498 BG11 medium (**Rippka et al., 1979**) supplemented with 5 mM NaHCO₃. Precultures were
499 cultivated in shaking flasks at 30-50 μE at 125 rpm (27 °C). Main cultures were cultivated in
500 500-700 mL BG11 at 27 °C in flasks which were either aerated with air or air supplemented
501 with 2 % CO₂. For this purpose, cultures were inoculated with an optical density (OD₇₅₀) of 0.2-
502 0.5 and then cultivated for the first three days at 10 μE (Lumilux de Lux, Daylight, Osram).
503 Later, the light intensity was set to around 30 μE. Growth was determined by measuring the
504 optical density at 750 nm (Specord 205, Analytik Jena). For feeding experiments the cultures
505 were supplemented at the beginning of the cultivation with 5dR, [U-¹³C₅]-5dR or
506 5-deoxyadenosine (5dAdo; Carbosynth Ltd.) at the respective concentrations (see Results
507 section). The other cyanobacterial strains (*Synechococcus* sp. PCC 6301, *Synechococcus* sp.
508 PCC 6312, *Synechococcus* sp. PCC 7502, *Synechocystis* sp. PCC 6803, *Anabaena variabilis*
509 ATCC 29413, *Nostoc punctiforme* ATCC 29133, *Anabaena* sp. PCC 7120) were cultivated as
510 described above. *Synechococcus* sp. PCC 7002 was cultivated in a 1:1 mixture of BG11 and
511 ASN III + vitamin B₁₂ (10 μg/mL) (**Rippka et al., 1979**).

512 *Streptomyces setonensis* SF666 was cultivated for 7 days as described in our previous work
513 (**Brilisaer et al., 2019**).

514

515 **Chemical synthesis of 5-deoxyribose and 7-deoxysedoheptulose (7dSh)**

516 5dR and [U-¹³C₅]-5dR **5** were synthesized in a four-step synthesis based on literature (**Sairam**
517 **et al., 2003; Zhang et al., 2013**) with additional optimization. All synthetic intermediates
518 shown in the reaction scheme (Figure S5) were verified by thin layer chromatography (TLC),
519 mass spectrometry and NMR. Detailed data for the ¹³C-labelled compounds are presented in
520 the Supplementary information. The synthesis starts with the reaction of D-ribose (Sigma) or
521 [U-¹³C₅]-D-ribose **1** (500.1 mg, 3.22 mmol; Eurisotop) in a 4:1 mixture of acetone:methanol
522 with SnCl₂·2 H₂O (1 eq) and catalytic amounts of conc. H₂SO₄ at 45 °C for 20 h. After cooling
523 to room temperature, the mixture was filtered, neutralised with NaHCO₃ solution, once again
524 filtered and the organic solvent was evaporated. The remaining aqueous solution was

525 extracted with ethylacetate, dried over Na₂SO₄ and evaporated in vacuo to yield the
526 acetonide-protected ribose **2** as a colourless oil (399.7 mg, 1.91 mmol, 59 %).

527 Envisaging the following deoxygenation reaction, the protected pentose **2** (399.7 mg,
528 1.91 mmol) was diluted in DCM with addition of TEA (2.5 eq). After cooling on ice,
529 mesylchloride (2.5 eq) was slowly added and then stirred for 5 h on ice. The reaction mixture
530 was washed with 1 N HCl, ultrapure water, NaHCO₃ solution, NaCl solution and again with
531 ultrapure water. The organic solvent was dried over Na₂SO₄ and evaporated in vacuo to give
532 **3** as a yellowish oil (556.5 mg, 1.97 mmol, 103 %, mesylchloride as impurity), which becomes
533 crystalline at 4 °C.

534 For the reduction as the third step **3** (556.1 mg, 1.91 mmol, maximum educt amount) was
535 diluted in DMSO. After cooling on ice NaBH₄ (5 eq) was added slowly. Afterwards the reaction
536 mixture was heated slowly to 85 °C and reacting for 12 h. After cooling on ice, 5 % AcOH was
537 added to quench remaining NaBH₄. The aqueous solution was extracted with DCM, washed
538 with ultrapure water, dried over Na₂SO₄ and evaporated in vacuo (40 °C, 750 mbar) to get **4**
539 as a colourless oil (357.7 mg, 1.85 mmol, 86 %).

540 Deprotecting to the target **5** was achieved by diluting the acetonide-protected ω-deoxy-sugar
541 **4** (357.7 mg, 1.85 mmol) in 0.04 N H₂SO₄ and heating to 85 °C for 3 h. After cooling to room
542 temperature, the reaction mixture was neutralised with NaHCO₃ solution and evaporated by
543 lyophilisation. The final product was first purified by MPLC (Gradient: start CHCl₃:MeOH 10:0;
544 end CHCl₃:MeOH 7:3) and HPLC (Column: HiPlexCa, 85 °C, 250x10.7 mm, 1.5 mL/min, solvent:
545 ultrapure water) to get [U-¹³C₅]-5-deoxy-D-ribofuranose (**5**) as a colourless oil (115.7 mg,
546 1.12 mmol, 61 %).

547 7dSh or [3,4,5,6,7-¹³C₅]-7dSh were synthesized in a transketolase based reaction with 5dR or
548 [U-¹³C₅]-5dR as substrate as described in our previous publication (*Brilisauer et al., 2019*) with
549 slight modifications: The reaction was performed in water instead of HEPES buffer, to ensure
550 an enhanced stability of hydroxypyruvate (very instable in HEPES (*Kobori et al., 1992*)). The
551 reaction was performed for 7 days and fresh hydroxypyruvate was added every day.
552 Purification was done as described for 5dR.

553 **Construction of insertion mutants**

554 To create an insertion mutant of the 5'-methylthioadenosine phosphorylase (EC: 2.4.2.28,
555 MtnP, *Synpcc7942_0932*) and of the glucose 1-phosphate phosphatase (EC: 3.1.3.10,
556 *Synpcc7942_1005*) in *S. elongatus* PCC 7942 a spectinomycin resistance cassette was
557 introduced inside the respective gene. An integrative plasmid was constructed in *E. coli* and
558 then transformed into *S. elongatus*. For this purpose, flanking regions on both sides of the
559 respective gene were amplified from *S. elongatus* colonies with primers adding an overlapping
560 fragment (46_0923_up_fw, 47_0923_up_rev and 48_Δ0923_down_fw, 49_0923_down_rev
561 for *Synpcc7942_0923::spec_R*; 85_1005_up_fw, 86_1005_up_rev and 87_1005_down_fw,
562 88_1005_down_rev for *Synpcc7942_1005::spec_R*). The primer sequences are shown in
563 Table S3. The spectinomycin resistance cassette was amplified with the primers 32_Spec_fw
564 and 33_Spec_rev from a plasmid containing the resistance cassette. All PCR amplification
565 products were introduced into a pUC19 vector cut with XbaI and PstI by using Gibson assembly
566 (**Gibson, 2011**). The plasmid was verified by Sanger sequencing (Eurofins Genomics). The
567 plasmid was then transformed into *S. elongatus* using natural competence. In short,
568 *S. elongatus* cells were harvested by centrifugation, washed with 400 μL BG11 and then
569 incubated with 1 μg DNA in the dark for 6 h (28 °C). The cells were then plated on BG11 agar
570 plates containing 10 μg/mL spectinomycin for three days. After that, the cells were transferred
571 to agar plates containing 20 μg/mL spectinomycin. Segregation was confirmed by colony PCR
572 (50_0923_rev_seg, 51_0923_fw_seg for *Synpcc7942_0923::spec_R*; 85_1005_up_fw,
573 88_1005_down_rev for *Synpcc7942_1005::spec_R*). Precultures of these strains, in the
574 following named as *S. elongatus mtnP::spec_R* or *S. elongatus 1005::spec_R* were cultivated in
575 the presence of 20 μg/mL spectinomycin. Main cultures were cultivated without antibiotic.

576

577 **Quantification of metabolites in the culture supernatant via GC-MS**

578 Culture supernatant was collected by centrifugation of 1.5 mL culture (16.000 x g, 10 min,
579 4 °C). 200 μL of the supernatant were transferred into a 2 mL reaction tube and immediately
580 frozen on liquid nitrogen and stored at -80 °C. The supernatant was lyophilized. For
581 intracellular measurements, the cell pellets were also frozen in liquid nitrogen. The samples
582 were extracted with 700 μL precooled CHCl₃/MeOH/H₂O (1/2.5/0.5 v/v/v) as described in the
583 literature (**Fürtauer et al., 2016**) with slight modifications. Samples were homogenized by

584 vortexing, ultrasonic bath (Bandelin, Sonorex) treatment (10 min) and shaking (10 min,
585 1.000 rpm). After that, the samples were cooled on ice for 5 min and then centrifuged (10 min,
586 16.000 x *g*, 4 °C). The supernatant was transferred into a new reaction tube. The pellet was
587 again extracted with 300 µL extraction solvent as described before. The supernatants were
588 pooled and 300 µL ice cold water was added for phase separation. The samples were vortexed,
589 incubated on ice (5 min) and then centrifuged (10 min, 16.000 x *g*, 4 °C). 900 µL of the upper,
590 polar phase were transferred into a new 2 mL reaction tube and dried in a vacuum
591 concentrator (Eppendorf, Concentrator plus, mode: V-AQ, 30 °C) for approximately 4.5 h. The
592 samples were immediately closed and then derivatized as described in the literature
593 (**Weckwerth et al., 2004**) with slight modifications. Therefore, the pellets were resolved in
594 60 µL methoxylamine hydrochloride (Acros Organics) in pyridine (anhydrous, Sigma-Aldrich)
595 (20 mg/mL), homogenized by vortexing, a treatment in an ultrasonic bath (15 min, RT) and an
596 incubation at 30 °C on a shaker (1.400 rpm) for 1.5 h. After that, 80 µL *N*-methyl-*N*-
597 (trimethylsilyl)trifluoroacetamide (MSTFA, Macherey-Nagel) was added and the samples were
598 incubated at 37 °C for 30 min (1.200 rpm). The samples were centrifuged (16.000 x *g*, 2 min)
599 and 120 µL were transferred into a glass vial with micro insert. The samples were stored at
600 room temperature for 2 h before GC-MS measurement.

601 GC-MS measurements were performed on a Shimadzu GC-MS TQ 8040 (Injector: AOC-20i,
602 Sampler: AOC-20s) with a SH-Rxi-5Sil-MS column (Restek, 30 m, 0.25 mm ID, 0.25 µm). For GC
603 measurement, the initial oven temperature was set to 60 °C for 3 min. After that the
604 temperature was increased by 10 °C/min up to 320 °C, which was then held for 10 min. The
605 GC-MS interface temperature was set to 280 °C, the ion source was heated to 200 °C. The
606 carrier gas flow (helium) was 1.28 mL/min. The injection was performed in split mode 1:10.
607 The mass spectrometer was operated in EI mode. Metabolites were detected in MRM mode.
608 Quantification of the metabolites was performed with a calibration curve of the respective
609 substances (5dAdo, 5dR, 7dSh, ¹³C₅-5dR, ¹³C₅-7dSh).

610

611 **Quantification of MTA and 5dAdo**

612 For the quantification of MTA and 5dAdo (Figure 6 E) 25 µL of culture supernatant were mixed
613 with 75 µL aqueous solution of 20 % MeOH (v/v) + 0.1 % (v/v) formic acid. Samples were
614 analysed on a LC-HR-MS system (Dionex Ultimate 3000 HPLC system coupled to maXis 4G

615 ESI-QTOF mass spectrometer). 5dAdo and MTA were separated on a C18 column with a
616 MeOH/H₂O gradient (10 %-100 % in 20 min). The concentration was calculated from peak
617 areas of extracted ion chromatograms of a calibration curve of the respective standards (MTA
618 was obtained from Cayman Chemicals).

619

620 **Crude Extract Assays**

621 Crude extract assays were performed by harvesting *S. elongatus* or *S. elongatus mtnP::spec_R*
622 cultures which were cultivated at 2 % CO₂ supplementation until an optical density of around
623 OD₇₅₀=4 (t=14 d). 10 mL of the cultures were centrifuged (3.200 x *g*, 10 min, 4 °C), the
624 supernatant was discarded, the pellet was washed with 10 mL fresh BG11 medium, and again
625 centrifuged. After that, the pellet was resuspended in 2.5 mL lysis buffer (25 mM HEPES
626 pH 7.5, 50 mM KCl, 1 mM DTT) and filled into 2 mL tubes with a screw cap. 100 µL glass beads
627 (∅=0.1-0.11 mm) was added and the cells were then disrupted at 4 °C by a FastPrep®-24
628 instrument (MP Biomedicals, 5 m/s, 20 sec, 3x with 5 min break). To remove the cell debris a
629 centrifugation step was performed (25.000 x *g*, 10 min, 4 °C). 200 µL of the supernatant was
630 used for the crude extract assay. The extract was either used alone or supplemented with
631 10 µL 5 mM 5dAdo (final concentration: 250 µM) or in combination with 40 µl 50 mM
632 potassium phosphate buffer (PBB) pH 7.5 (final concentration: 10 mM). The extracts were
633 incubated at 28 °C for 7 h, then frozen in liquid nitrogen and lyophilized. 100 µL MeOH was
634 added, the samples were homogenized and then centrifuged. 50 µL was applied on a TLC plate
635 (ALUGRAM® Xtra SIL G UV₂₅₄, Macherey-Nagel). For the mobile phase CHCl₃/MeOH in a ratio
636 of 9:5 (v/v) with 1 % (v) formic acid was used. Visualization was performed at 254 nm
637 (Figure 7) or spraying with anisaldehyde (Figure S3).

638

639 **Bioinformatics**

640 Annotations of the different genes were obtained by the KEGG database (*Kanehisa and Goto,*
641 **2000**). Also, radical SAM enzyme search was done in KEGG database (searching for pf:
642 Radical_SAM, PF04055). Searching for homologous genes was performed by using BlastP
643 (BLOSUM 62). Searching for Ald2 homologs in KEGG database, *R. rubrum* protein sequence

644 (rru:Rru_A0359) was used as a query sequence and an e-value <10e-20 was used for positive
645 results.

646

647 **Author Contributions**

648 J. R. designed, performed, interpreted experiments, and wrote the manuscript. P. R.
649 synthesized labelled and unlabelled 5dR and 7dSh. J. K. optimized the GC-MS method and
650 supported with GC-MS measurements. K. B supported initial experiments and proof-read
651 manuscript. S. G. supported chemical analytics and proof-read manuscript. K. F. supervised
652 the study and supported manuscript writing.

653

654 **Acknowledgements**

655 Work of the authors is supported and funded by the “Glycobiotechnology” initiative (Ministry
656 for Science, Research and Arts Baden-Württemberg), the RTG 1708 “Molecular principles of
657 bacterial survival strategies” and the Institutional Strategy of the University of Tübingen
658 (Deutsche Forschungsgemeinschaft, ZUK 63). The work was further supported by
659 infrastructural funding from the DFG Cluster of Excellence EXC 2124 Controlling Microbes to
660 Fight Infections. We thank Dr. Libera Lo Presti for critical reading the manuscript. We
661 especially thank Tim Orthwein for fruitful discussions and Michaela Schuppe for the cultivation
662 of *Streptomyces setonensis*.

663

664 **Competing interests**

665 The authors declare no competing interests.

666 References

- 667 **Abuaita BH**, Withey JH. 2009. Bicarbonate Induces *Vibrio cholerae* virulence gene expression
668 by enhancing ToxT activity. *Infection and Immunity* **77**:4111–4120. doi: 10.1128/IAI.00409-
669 09.
- 670 **Albers E**. 2009. Metabolic characteristics and importance of the universal methionine
671 salvage pathway recycling methionine from 5'-methylthioadenosine. *IUBMB Life* **61**:1132–
672 1142. doi: 10.1002/iub.278.
- 673 **Beaudoin GAW**, Li Q, Folz J, Fiehn O, Goodsell JL, Angerhofer A, Bruner SD, Hanson AD. 2018.
674 Salvage of the 5-deoxyribose byproduct of radical SAM enzymes. *Nature Communications*
675 **9**:3105. doi: 10.1038/s41467-018-05589-4.
- 676 **Blombach B**, Takors R. 2015. CO₂ - Intrinsic Product, Essential Substrate, and Regulatory
677 Trigger of Microbial and Mammalian Production Processes. *Frontiers in Bioengineering*
678 *and Biotechnology* **3**. doi: 10.3389/fbioe.2015.00108.
- 679 **Booker SJ**, Grove TL. 2010. Mechanistic and functional versatility of radical SAM enzymes.
680 *F1000 Biology Reports* **2**:52. doi: 10.3410/B2-52.
- 681 **Brilisauer K**, Rapp J, Rath P, Schöllhorn A, Bleul L, Weiß E, Stahl M, Grond S, Forchhammer K.
682 2019. Cyanobacterial antimetabolite 7-deoxy-sedoheptulose blocks the shikimate
683 pathway to inhibit the growth of prototrophic organisms. *Nature Communications* **10**:545.
684 doi: 10.1038/s41467-019-08476-8.
- 685 **Broderick JB**, Duffus BR, Duschene KS, Shepard EM. 2014. Radical S-adenosylmethionine
686 enzymes. *Chemical Reviews* **114**:4229–4317. doi: 10.1021/cr4004709.
- 687 **Burnap RL**, Hagemann M, Kaplan A. 2015. Regulation of CO₂ Concentrating Mechanism in
688 Cyanobacteria. *Life* **5**:348–371. doi: 10.3390/life5010348.
- 689 **Burroughs AM**, Allen KN, Dunaway-Mariano D, Aravind L. 2006. Evolutionary genomics of
690 the HAD superfamily: understanding the structural adaptations and catalytic diversity in a
691 superfamily of phosphoesterases and allied enzymes. *Journal of Molecular Biology*
692 **361**:1003–1034. doi: 10.1016/j.jmb.2006.06.049.
- 693 **Challand MR**, Ziegert T, Douglas P, Wood RJ, Kriek M, Shaw NM, Roach PL. 2009. Product
694 inhibition in the radical S-adenosylmethionine family. *FEBS Letters* **583**:1358–1362.
695 doi: 10.1016/j.febslet.2009.03.044.
- 696 **Chattopadhyay MK**, Tabor CW, Tabor H. 2006. Methylthioadenosine and polyamine
697 biosynthesis in a *Saccharomyces cerevisiae* *meu1Δ* mutant. *Biochemical and Biophysical*
698 *Research Communications* **343**:203–207. doi: 10.1016/j.bbrc.2006.02.144.
- 699 **Choi-Rhee E**, Cronan JE. 2005. A Nucleosidase Required for In Vivo Function of the S-
700 Adenosyl-L-Methionine Radical Enzyme, Biotin Synthase. *Chemistry & Biology* **12**:589–593.
701 doi: 10.1016/j.chembiol.2005.04.012.
- 702 **Copeland A**, Lucas S, Lapidus A, Barry K, Detter JC, Glavina T, Hammon N, Israni S, Pitluck S,
703 Schmutz J, Larimer F, Land, M M, Kyrpides N, Lykidis A, Golden S, Richardson P. 2014.
704 Complete sequence of chromosome 1 of *Synechococcus elongatus* PCC 7942.
- 705 **Farrar CE**, Siu KKW, Howell PL, Jarrett JT. 2010. Biotin synthase exhibits burst kinetics and
706 multiple turnovers in the absence of inhibition by products and product-related
707 biomolecules. *Biochemistry* **49**:9985–9996. doi: 10.1021/bi101023c.
- 708 **Fontecave M**, Atta M, Mulliez E. 2004. S-adenosylmethionine: nothing goes to waste. *Trends*
709 *in Biochemical Sciences* **29**:243–249. doi: 10.1016/j.tibs.2004.03.007.
- 710 **Fürtauer L**, Weckwerth W, Nägele T. 2016. A Benchtop Fractionation Procedure for
711 Subcellular Analysis of the Plant Metabolome. *Frontiers in Plant Science* **7**.
712 doi: 10.3389/fpls.2016.01912.

- 713 **Gibson DG**. 2011. Enzymatic Assembly of Overlapping DNA Fragments. In: Voigt C, ed.
714 *Methods in Enzymology: Synthetic Biology, Part B*. Academic Press.
- 715 **Golden SS**. 2019. The international journeys and aliases of *Synechococcus elongatus*. *New*
716 *Zealand Journal of Botany* **57**:70–75. doi: 10.1080/0028825X.2018.1551805.
- 717 **Herter T**, Berezina OV, Zinin NV, Velikodvorskaya GA, Greiner R, Borriss R. 2006. Glucose-1-
718 phosphatase (AgpE) from *Enterobacter cloacae* displays enhanced phytase activity.
719 *Applied Microbiology and Biotechnology* **70**:60–64. doi: 10.1007/s00253-005-0024-8.
- 720 **Holliday GL**, Akiva E, Meng EC, Brown SD, Calhoun S, Pieper U, Sali A, Booker SJ, Babbitt PC.
721 2018. Atlas of the Radical SAM Superfamily: Divergent Evolution of Function Using a “Plug
722 and Play” Domain. *Methods in Enzymology* **606**:1–71. doi: 10.1016/bs.mie.2018.06.004.
- 723 **Hughes JA**. 2006. In vivo hydrolysis of S-adenosyl-L-methionine in *Escherichia coli* increases
724 export of 5-methylthioribose. *Canadian Journal of Microbiology* **52**:599–602.
725 doi: 10.1139/w06-008.
- 726 **Ito T**, Ezaki N, Tsuruoka T, Niida T. 1971. Structure of SF-666 A and SF-666 B, new
727 monosaccharides. *Carbohydrate Research* **17**:375–382. doi: 10.1016/S0008-
728 6215(00)82545-8.
- 729 **Kamatani N**, Carson DA. 1980. Abnormal regulation of methylthioadenosine and polyamine
730 metabolism in methylthioadenosine phosphorylase-deficient human leukemic cell lines.
731 *Cancer Research* **40**:4178–4182.
- 732 **Kanehisa M**, Goto S. 2000. KEGG: Kyoto Encyclopedia of Genes and Genomes. *Nucleic Acids*
733 *Research* **28**:27–30. doi: 10.1093/nar/28.1.27.
- 734 **Kobori Y**, Myles DC, Whitesides GM. 1992. Substrate specificity and carbohydrate synthesis
735 using transketolase. *The Journal of Organic Chemistry* **57**:5899–5907.
736 doi: 10.1021/jo00048a023.
- 737 **Koonin EV**, Tatusov RL. 1994. Computer analysis of bacterial haloacid dehalogenases defines
738 a large superfamily of hydrolases with diverse specificity. Application of an iterative
739 approach to database search. *Journal of Molecular Biology* **244**:125–132.
740 doi: 10.1006/jmbi.1994.1711.
- 741 **Kuznetsova E**, Proudfoot M, Gonzalez CF, Brown G, Omelchenko MV, Borozan I, Carmel L,
742 Wolf YI, Mori H, Savchenko AV, Arrowsmith CH, Koonin EV, Edwards AM, Yakunin AF.
743 2006. Genome-wide analysis of substrate specificities of the *Escherichia coli* haloacid
744 dehalogenase-like phosphatase family. *The Journal of Biological Chemistry* **281**:36149–
745 36161. doi: 10.1074/jbc.M605449200.
- 746 **Lee JE**, Settembre EC, Cornell KA, Riscoe MK, Sufrin JR, Ealick SE, Howell PL. 2004. Structural
747 comparison of MTA phosphorylase and MTA/AdoHcy nucleosidase explains substrate
748 preferences and identifies regions exploitable for inhibitor design. *Biochemistry* **43**:5159–
749 5169. doi: 10.1021/bi035492h.
- 750 **Li B**, Sher D, Kelly L, Shi Y, Huang K, Knerr PJ, Joewono I, Rusch D, Chisholm SW, van der Donk
751 WA. 2010. Catalytic promiscuity in the biosynthesis of cyclic peptide secondary
752 metabolites in planktonic marine cyanobacteria. *Proceedings of the National Academy of*
753 *Sciences* **107**:10430–10435. doi: 10.1073/pnas.0913677107.
- 754 **Ma L**, Bartholome A, Tong MH, Qin Z, Yu Y, Shepherd T, Kyeremeh K, Deng H, O'Hagan D.
755 2015. Identification of a fluorometabolite from *Streptomyces* sp. MA37: (2R3S4S)-5-fluoro-
756 2,3,4-trihydroxypentanoic acid. *Chemical Science* **6**:1414–1419. doi: 10.1039/C4SC03540B.
- 757 **Marsh ENG**, Patterson DP, Li L. 2010. Adenosyl Radical: Reagent and Catalyst in Enzyme
758 Reactions. *ChemBioChem* **11**:604–621. doi: 10.1002/cbic.200900777.

- 759 **Miller DV**, Rauch BJ, Harich K, Xu H, Perona JJ, White RH. 2018. Promiscuity of methionine
760 salvage pathway enzymes in *Methanocaldococcus jannaschii*. *Microbiology* **164**:969–981.
761 doi: 10.1099/mic.0.000670.
- 762 **North JA**, Wildenthal JA, Erb TJ, Evans BS, Byerly KM, Gerlt JA, Tabita FR. 2020. A bifunctional
763 salvage pathway for two distinct *S*-adenosylmethionine by-products that is widespread in
764 bacteria, including pathogenic *Escherichia coli*. *Molecular Microbiology* **113**:923–937.
765 doi: 10.1111/mmi.14459.
- 766 **Palmer LD**, Downs DM. 2013. The thiamine biosynthetic enzyme ThiC catalyzes multiple
767 turnovers and is inhibited by *S*-adenosylmethionine (AdoMet) metabolites. *Journal of*
768 *Biological Chemistry* **288**:30693–30699. doi: 10.1074/jbc.M113.500280.
- 769 **Parveen N**, Cornell KA. 2011. Methylthioadenosine/*S*-adenosylhomocysteine nucleosidase, a
770 critical enzyme for bacterial metabolism. *Molecular Microbiology* **79**:7–20.
771 doi: 10.1111/j.1365-2958.2010.07455.x.
- 772 **Plagemann PG**, Wohlueter RM. 1983. 5'-Deoxyadenosine metabolism in various
773 mammalian cell lines. *Biochemical Pharmacology* **32**:1433–1440. doi: 10.1016/0006-
774 2952(83)90458-6.
- 775 **Pradel E**, Boquet PL. 1988. Acid phosphatases of *Escherichia coli*: molecular cloning and
776 analysis of *agg*, the structural gene for a periplasmic acid glucose phosphatase. *Journal of*
777 *Bacteriology* **170**:4916–4923. doi: 10.1128/jb.170.10.4916-4923.1988.
- 778 **Rippka R**, Deruelles J, Waterbury JB, Herdman M, Stanier RY. 1979. Generic Assignments,
779 Strain Histories and Properties of Pure Cultures of Cyanobacteria. *Journal of General*
780 *Microbiology* **111**:1–61. doi: 10.1099/00221287-111-1-1.
- 781 **Rossi F**, Philippis R de. 2015. Role of cyanobacterial exopolysaccharides in phototrophic
782 biofilms and in complex microbial mats. *Life* **5**:1218–1238. doi: 10.3390/life5021218.
- 783 **Sairam P**, Puranik R, Sreenivasa Rao B, Veerabhadra Swamy P, Chandra S. 2003. Synthesis of
784 1,2,3-tri-*O*-acetyl-5-deoxy-*D*-ribofuranose from *D*-ribose. *Carbohydrate Research* **338**:303–
785 306. doi: 10.1016/S0008-6215(02)00464-0.
- 786 **Savarese TM**, Crabtree GW, Parks RE. 1981. 5'-methylthioadenosine phosphorylase—I:
787 Substrate activity of 5'-deoxyadenosine with the enzyme from Sarcoma 180 cells.
788 *Biochemical Pharmacology* **30**:189–199. doi: 10.1016/0006-2952(81)90077-0.
- 789 **Schroeder HR**, Barnes CJ, Bohinski RC, Mumma RO, Mallette MF. 1972. Isolation and
790 identification of 5-methylthioribose from *Escherichia coli* B. *Biochimica et Biophysica Acta*
791 *(BBA) - General Subjects* **273**:254–264. doi: 10.1016/0304-4165(72)90215-2.
- 792 **Sekowska A**, Ashida H, Danchin A. 2018. Revisiting the methionine salvage pathway and its
793 paralogues. *Microbial Biotechnology* **12**:77–97. doi: 10.1111/1751-7915.13324.
- 794 **Sekowska A**, Danchin A. 2002. The methionine salvage pathway in *Bacillus subtilis*. *BMC*
795 *Microbiology* **2**:8. doi: 10.1186/1471-2180-2-8.
- 796 **Sekowska A**, Denervaud V, Ashida H, Michoud K, Haas D, Yokota A, Danchin A. 2004.
797 Bacterial variations on the methionine salvage pathway. *BMC Microbiology* **4**:9.
798 doi: 10.1186/1471-2180-4-9.
- 799 **Selim KA**, Haase F, Hartmann MD, Hagemann M, Forchhammer K. 2018. P_{II}-like signaling
800 protein SbtB links cAMP sensing with cyanobacterial inorganic carbon response.
801 *Proceedings of the National Academy of Sciences* **115**:E4861–E4869.
802 doi: 10.1073/pnas.1803790115.
- 803 **Shih PM**, Wu D, Latifi A, Axen SD, Fewer DP, Talla E, Calteau A, Cai F, Tandeau de Marsac N,
804 Rippka R, Herdman M, Sivonen K, Coursin T, Laurent T, Goodwin L, Nolan M, Davenport
805 KW, Han CS, Rubin EM, Eisen JA, Woyke T, Gugger M, Kerfeld CA. 2013. Improving the
806 coverage of the cyanobacterial phylum using diversity-driven genome sequencing.

- 807 *Proceedings of the National Academy of Sciences* **110**:1053–1058.
808 doi: 10.1073/pnas.1217107110.
- 809 **Sofia HJ**, Chen G, Hetzler BG, Reyes-Spindola JF, Miller NE. 2001. Radical SAM, a novel
810 protein superfamily linking unresolved steps in familiar biosynthetic pathways with radical
811 mechanisms: Functional characterization using new analysis and information visualization
812 methods. *Nucleic Acids Research* **29**:1097–1106. doi: 10.1093/nar/29.5.1097.
- 813 **Sugita C**, Ogata K, Shikata M, Jikuya H, Takano J, Furumichi M, Kanehisa M, Omata T, Sugiura
814 M, Sugita M. 2007. Complete nucleotide sequence of the freshwater unicellular
815 cyanobacterium *Synechococcus elongatus* PCC 6301 chromosome: gene content and
816 organization. *Photosynthesis Research* **93**:55–67. doi: 10.1007/s11120-006-9122-4.
- 817 **Suleimanova AD**, Beinbauer A, Valeeva LR, Chastukhina IB, Balaban NP, Shakirov EV, Greiner
818 R, Sharipova MR. 2015. Novel Glucose-1-Phosphatase with High Phytase Activity and
819 Unusual Metal Ion Activation from Soil Bacterium *Pantoea* sp. Strain 3.5.1. *Applied and
820 Environmental Microbiology* **81**:6790–6799. doi: 10.1128/AEM.01384-15.
- 821 **Turner DH**, Turner JF. 1960. The hydrolysis of glucose monophosphates by a phosphatase
822 preparation from pea seeds. *Biochemical Journal* **74**:486–491. doi: 10.1042/bj0740486.
- 823 **Wang SC**, Frey PA. 2007. S-adenosylmethionine as an oxidant: the radical SAM superfamily.
824 *Trends in Biochemical Sciences* **32**:101–110. doi: 10.1016/j.tibs.2007.01.002.
- 825 **Weckwerth W**, Wenzel K, Fiehn O. 2004. Process for the integrated extraction, identification
826 and quantification of metabolites, proteins and RNA to reveal their co-regulation in
827 biochemical networks. *Proteomics* **4**:78–83. doi: 10.1002/pmic.200200500.
- 828 **Wray JW**, Abeles RH. 1995. The methionine salvage pathway in *Klebsiella pneumoniae* and
829 rat liver. Identification and characterization of two novel dioxygenases. *The Journal of
830 Biological Chemistry* **270**:3147–3153. doi: 10.1074/jbc.270.7.3147.
- 831 **Yang Y**, Lam V, Adomako M, Simkovsky R, Jakob A, Rockwell NC, Cohen SE, Taton A, Wang J,
832 Lagarias JC, Wilde A, Nobles DR, Brand JJ, Golden SS. 2018. Phototaxis in a wild isolate of
833 the cyanobacterium *Synechococcus elongatus*. *Proceedings of the National Academy of
834 Sciences* **115**:E12378–E12387. doi: 10.1073/pnas.1812871115.
- 835 **Zappia V**, Della Ragione F, Pontoni G, Gragnaniello V, Carteni-Farina M. 1988. Human 5'-
836 Deoxy-5'-Methylthioadenosine Phosphorylase: Kinetic Studies and Catalytic Mechanism.
837 In: Zappia V, Pegg AE, eds. *Progress in Polyamine Research: Novel Biochemical,
838 Pharmacological, and Clinical Aspects*. Springer US, Boston, MA.
- 839 **Zhang JT**, Chen SP, Feng JM, Liu DW, Tang LJ, Wang XJ, Huang SP. 2013. Synthetic Study of 1,
840 2, 3-Tri-O-Acetyl-5-Deoxy-D-Ribofuranose. *Advanced Materials Research* **781-784**:1184–
841 1186. doi: 10.4028/www.scientific.net/AMR.781-784.1184.